

Electronic Supplementary Information for

Bipolar doping and thermoelectric properties of Zintl arsenide

$\text{Eu}_5\text{In}_2\text{As}_6$

Naoki Tomitaka,^a Yosuke Goto,^{*a} Kota Morino,^a Kazuhisa Hoshi,^a Yuki Nakahira,^a
Hiroaki Ito,^b Akira Miura,^b Hidetomo Usui,^{*c} Yoshikazu Mizuguchi^a

^a*Department of Physics, Tokyo Metropolitan University, 1-1 Minami-osawa, Hachioji, Tokyo 192-0397, Japan*

^b*Faculty of Engineering, Hokkaido University, Kita 13, Nishi 8 Sapporo 060-8628, Japan*

^c*Department of Physics and Materials Science, Shimane University, Matsue, 690-8504, Japan*

e-mail: y_goto@tmu.ac.jp, hidetomo.usui@riko.shimane-u.ac.jp

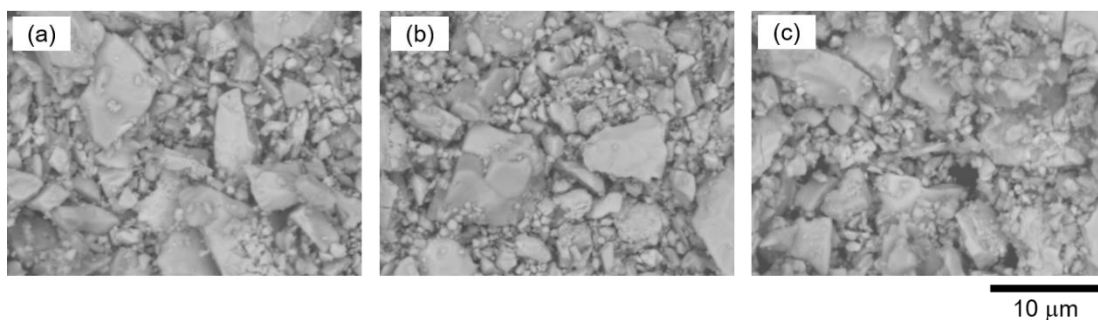


Figure S1. SEM images of pulverized powder of (a) $\text{Eu}_5\text{In}_2\text{As}_6$, (b) $\text{Eu}_{4.90}\text{La}_{0.10}\text{In}_2\text{As}_6$, and (c) $\text{Eu}_5\text{In}_{1.90}\text{Zn}_{0.10}\text{As}_6$.

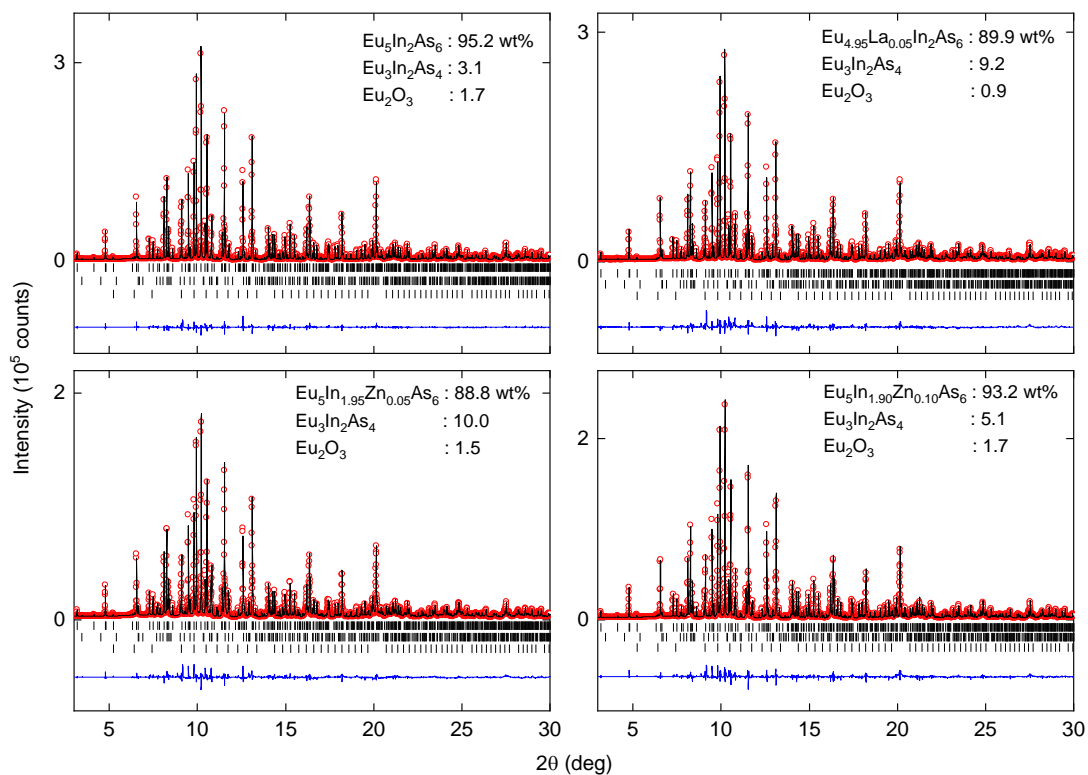


Figure S2

Observed synchrotron X-ray diffraction pattern and the Rietveld refinement results. The circles (red) and solid lines (black) represent the observed and calculated patterns, respectively. The difference between the observed and calculated patterns is shown at the bottom (blue). The vertical marks indicate the Bragg reflection positions for $\text{Eu}_5\text{In}_2\text{As}_6$ -type phase, $\text{Eu}_3\text{In}_2\text{As}_4$, and Eu_2O_3 , respectively, from top to bottom. Amount of these phases are denoted in the inset.

Table S1

Reliability factors of the Rietveld refinement of $\text{Eu}_{5-x}\text{La}_x\text{In}_2\text{As}_6$ and $\text{Eu}_5\text{In}_{2-y}\text{Zn}_y\text{As}_6$.

Sample	R_{wp} (%)	R_{p} (%)	GOF
$\text{Eu}_{5-x}\text{La}_x\text{In}_2\text{As}_6$			
$x = 0$	5.37	5.17	7.17
0.05	8.70	7.92	11.17
0.10	8.35	6.78	9.70
$\text{Eu}_5\text{In}_{2-y}\text{Zn}_y\text{As}_6$			
$y = 0.05$	5.58	5.77	7.93
0.10	6.94	6.97	9.80

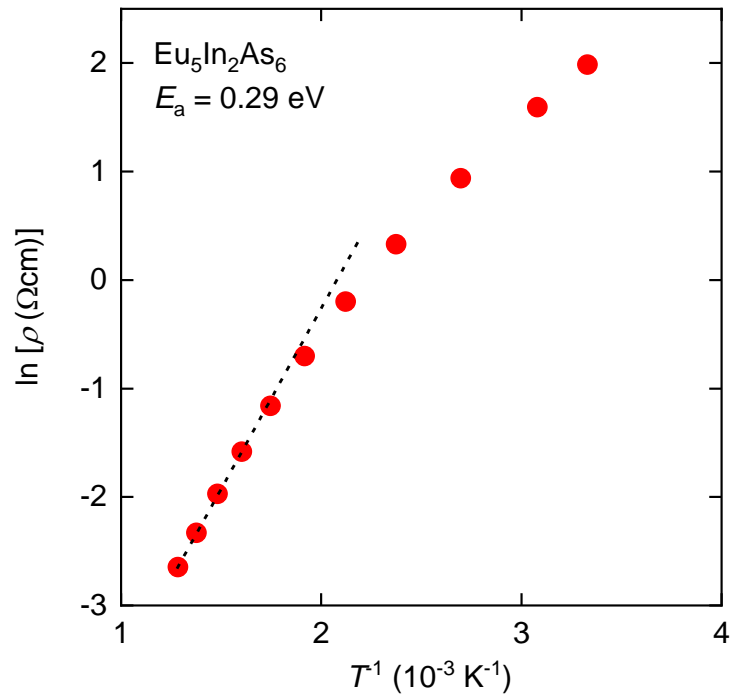


Figure S3

Temperature (T) dependence of electrical resistivity (ρ) of $\text{Eu}_5\text{In}_2\text{As}_6$. Activation energy (E_a) was obtained using measurement results from 623 to 778 K.

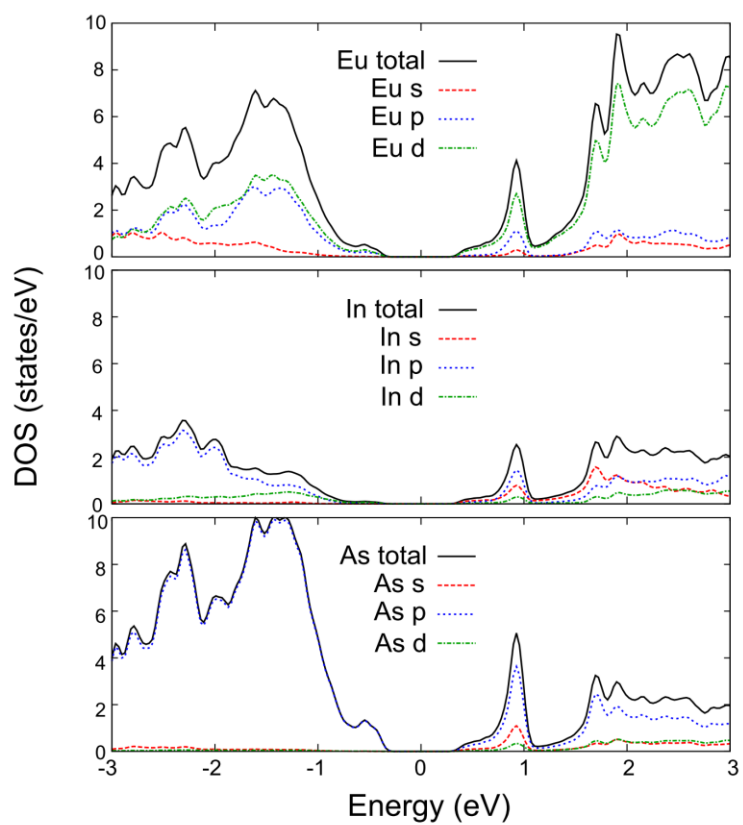


Figure S4
Partial density of states (DOS) of $\text{Eu}_5\text{In}_2\text{As}_6$.

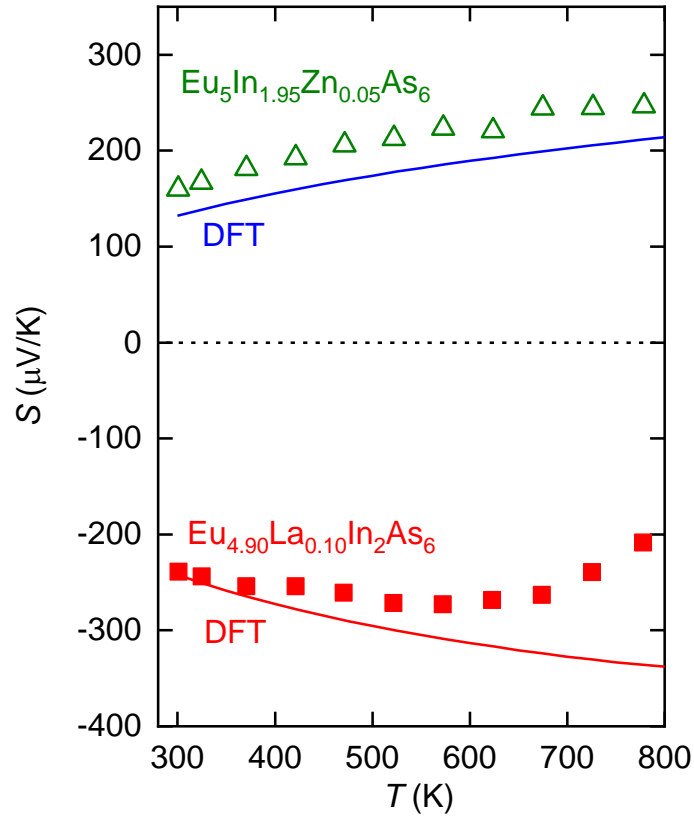


Figure S5

Temperature (T) dependence of Seebeck coefficient (S) of $\text{Eu}_5\text{In}_{1.95}\text{Zn}_{0.05}\text{As}_6$ and $\text{Eu}_{4.90}\text{La}_{0.10}\text{In}_2\text{As}_6$. Calculated S using density functional theory (DFT) is also shown. Measured hole concentration ($1.1 \times 10^{20} \text{ cm}^{-3}$) was used to plot calculated results for p-type region, while electron concentration of $1.6 \times 10^{19} \text{ cm}^{-3}$ was assumed for n-type region, because reliable Hall coefficient cannot be obtained for n-type La-doped samples.

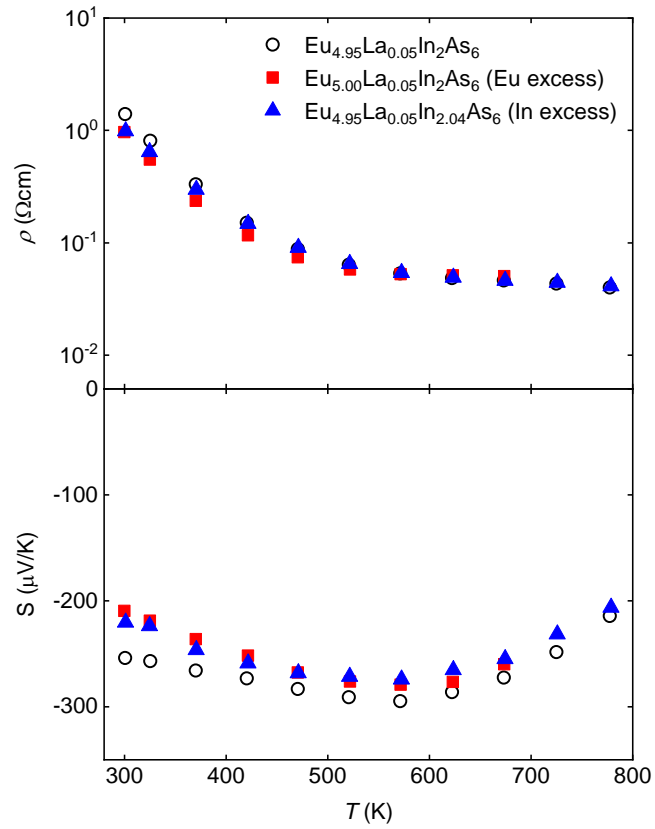


Figure S6

Temperature (T) dependence of electrical resistivity (ρ) and Seebeck coefficient (S) of La-doped $\text{Eu}_5\text{In}_2\text{As}_6$ synthesized with excess amount of Eu or La. Nominal composition of starting materials is denoted in the inset.